

Self-Folded Silyl Cavitands with In- and Outwardly Directed Allyl Groups

Kazuhiro Ohashi,^[a] Kouhei Ito,^[a] and Tetsuo Iwasawa*^[a]

Keywords: Supramolecular chemistry / Cavitands / Macrocycles / Silanes / Introverted functionality

Cavitands endowed with in- and outwardly directed allylsilanes are described; epoxidation reactions of the allyl groups with *meta*-chloroperbenzoic acid are included. The synthesis of introverted and extroverted allylsilanes tethered to triquinoxaline-spanned resorcinarenes was successfully

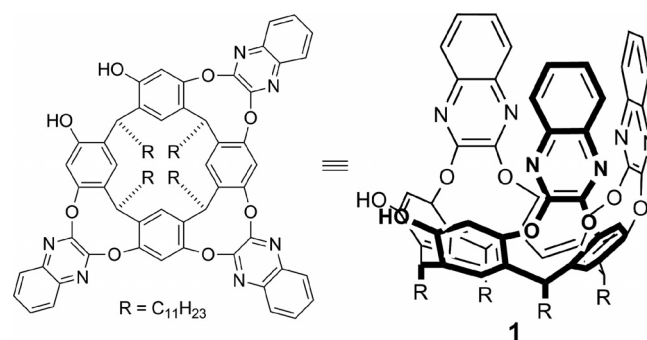
achieved. Competitive epoxidation experiments between the two isomers disclosed that the introverted allyl was more reactive than the extroverted allyl, despite a clearly congested nuisance: the vase-formed cavity would actively stabilize the reaction process.

Introduction

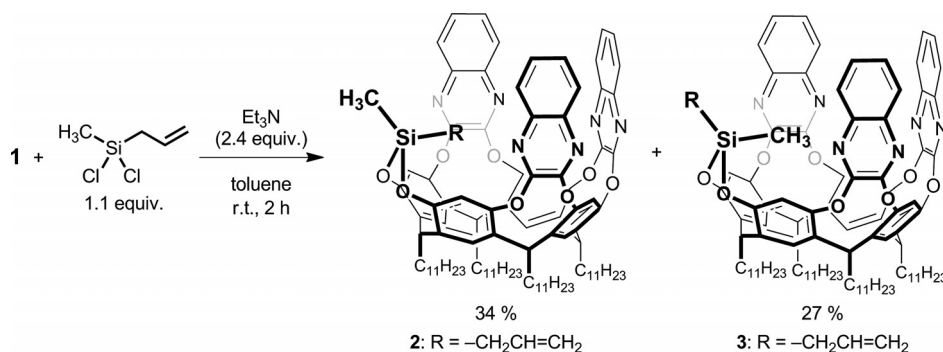
Natural supramolecular systems integrate inwardly directed functions. The binding sites of enzymes, polypeptides, and RNA strands can fold around a substrate, and in the folded state the functionality converges on the substrate.^[1,2] The introverted functionalities in biological macromolecules play quintessential roles in catalysis.^[3]

In a similar vein, a synthetic approach to the chemical space with introverted functionality has been pioneered,^[4–6] particularly by Rebek and co-workers.^[7] They use the deepened cavitand derived from Högberg's resorcinarene scaffold and four aromatic exteriors. The functional substituent is up in the interior space, like a fishing line, toward the tapered end. Indeed, there are many parallels between the synthetic and natural systems: the introverted function-

ality can recognize guests,^[8] accelerate^[9] and catalyze reactions,^[10] and stabilize reactive intermediates.^[11,12] Despite the relevant role played by inwardly functionalized cavit-



Scheme 1. Triquinoxaline-spanned resorcin[4]arene 1.



Scheme 2. Synthesis of cavitands 2 and 3.

[a] Department of Materials Chemistry, Faculty of Science and Technology, Ryukoku University, Seta, Otsu 520-2194, Japan
 E-mail: iwasawa@rins.ryukoku.ac.jp
<http://www.chem.ryukoku.ac.jp/iwasawa/index.html>
 Supporting information for this article is available on the WWW under <http://dx.doi.org/10.1002/ejoc.201301843>.

ands in supramolecular chemistry, the organization of reaction sites inside the space is underrepresented owing to the synthetic difficulty in functionalizing concave surfaces.^[13] To overcome this intrinsic problem would expand the possibilities and importance of functionalized cavitands.

Herein, we report a novel synthesis of self-folded silyl cavitands endowed with in- and outwardly directed allyl groups. The reactions of triquinoxaline-spanned cavitand **1** (Scheme 1) with allyl(dichloro)methylsilane yielded isomers of introverted allyl **2** and extroverted allyl **3** (Scheme 2). Analysis by NMR spectroscopy elucidated that the cavity of **2** definitely holds an allyl moiety; functionalizing the concave surfaces was successfully achieved. In addition, the two isomers underwent epoxidation with *meta*-chloroperbenzoic acid (*m*CPBA), and **2** was more reactive than **3** in competitive experiments.

Results and Discussion

We commenced the reaction of **1** with commercially available allyl(dichloro)methylsilane. The reactions proceeded smoothly in 2 h in toluene with complete consumption of **1** (Scheme 2). An isomeric mixture of **2** and **3** was obtained; the separation of **2** from **3** was a terribly pesky operation, because these compounds had nearly the same R_f values in several eluents. Employment of a large amount of silica gel gave separate fractions of single isomers of each **2** and **3** in 34 and 27% yield, respectively. As each ratio of **2/3** in the crude state was nearly comparable to 1:1, selective substitution reactions of the allyl(dichloro)methylsilane with **1** did not occur.

Portions of the ^1H NMR spectra of **2** and **3** in $[\text{D}_8]\text{toluene}$ are shown in Figure 1. The CH methine protons, which are located directly below the quinoxaline units, are situated in the mid-field region at $\delta = 6.14$, 6.05, and 4.77 ppm. These values indicate that the vase conformation was ensured.^[4c,14,15] It is possible to distinguish between **2** and **3**, because the magnetically shielded environment caused by the inner space shifts inwardly directed protons strongly upfield.^[16] The upfield portions near $\delta = 0$ ppm shows two sets of signals: H^a/H^b at $\delta = 0.28/-0.13$ ppm and H^a/H^b at $\delta = -1.32/1.66$ ppm. This indicates that H^b in the former and H^a in the latter are enclosed by the space; thus, the orientation of the substituents on the silicon atom was determined.

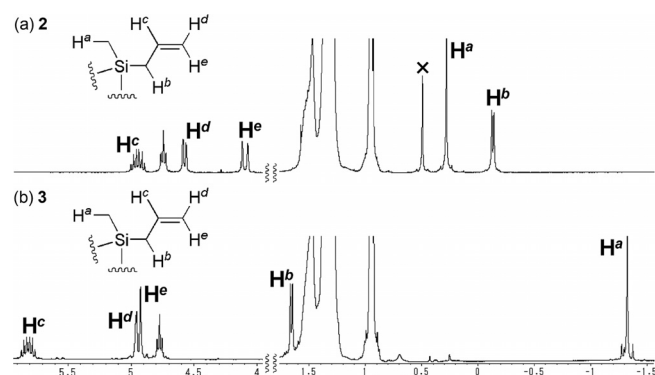
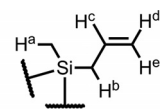


Figure 1. Mid- and upfield portions of the ^1H NMR spectra for (a) **2** and (b) **3** (400 MHz, $[\text{D}_8]\text{toluene}$). The resonance labelled with “x” corresponds to water.

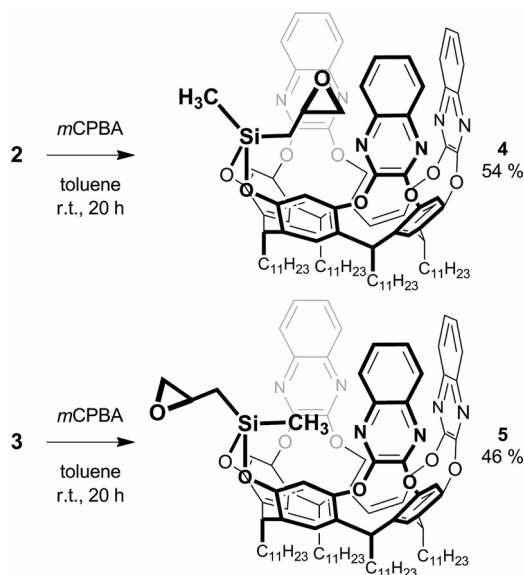
On the basis of the results in Figure 1, the difference in the chemical shifts ($\Delta\delta$ values) between **2** and **3** are summarized in Figure 2. The protons of the CH_2 and CH_3 groups directly bonded to the silicon atoms show relatively large values of approximately 1.7. This suggests that the closest position to the silicon atom is most sufficiently covered by the anisotropic effect of the strong π surrounding ended with the inner space. Interestingly, the H^d and H^e protons in the exo methylene unit showed quite different $\Delta\delta$ values: $\Delta\delta = 0.37$ for H^d is the smallest, and $\Delta\delta = 0.85$ for H^e is comparable with the value for H^c . This implies that in **2**, the H^d proton is outside the strong magnetically shielded environment, and this directs H^e to the concave portion of the shaped surface.



	H^a	H^b	H^c	H^d	H^e
$\Delta\delta$	+1.6	-1.8	-0.87	-0.37	-0.85

Figure 2. The differences in the chemical shifts ($\Delta\delta$) in $[\text{D}_8]\text{toluene}$ between the in- and outwardly directed allyl protons of **2** and **3**. The values are standardized as $(\delta \text{ of } \mathbf{2}) - (\delta \text{ of } \mathbf{3})$.

Scheme 3 illustrates epoxidation reactions of **2** and **3** (1 equiv.) with *m*CPBA (1 equiv.) in toluene. Almost all of the starting allyl compounds disappeared, as indicated by TLC monitoring, and both compounds underwent clean transformations. However, purification by column chromatography seemed to decrease the yield to 54% for **4** and to 46% for **5**. As depicted in Figure 3, the mid- and upfield portions of the ^1H NMR spectra of **4** and **5** in $[\text{D}_8]\text{toluene}$ show characteristic signatures of epoxide moieties with reasonable $\Delta\delta$ values. Specifically, the geminal protons of SiCH_2 for **4** are located at $\delta = -0.60$ ppm with $J = 15.4$ and 7.0 Hz and at $\delta = -0.8$ ppm with $J = 15.4$ and 5.4 Hz.



Scheme 3. Epoxidation of allylsilanes **2** and **3**.

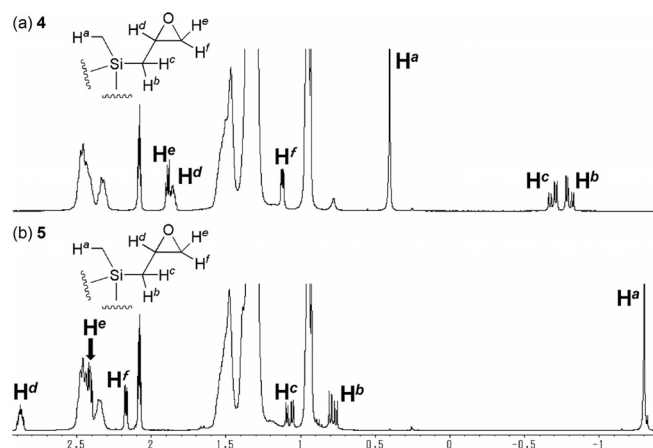


Figure 3. Upfield portion of the ^1H NMR spectra for (a) **4** and (b) **5** (400 MHz, $[\text{D}_8]\text{toluene}$).

With a workable protocol in hand, competitive reactions between **2** and **3** were evaluated through clean epoxidation (Table 1). The experiments in NMR tubes were performed in $[\text{D}_6]\text{benzene}$, $[\text{D}_8]\text{toluene}$, $[\text{D}_{10}]\text{-}p\text{-xylene}$, and $[\text{D}_{12}]\text{-mesitylene}$,^[15] and ratios of **4/5/2/3** are summarized. The ratios of **4/5** are around 30:20 through entries 1–3, and they are consistent with the conversions of **2** and **3**: in brief, **4** significantly exceeds **5** in yield.^[17] The reaction center of the allyl group in **2** is located at a more congested area than in **3** because the quinoxaline encapsulates the allyl, and therefore, smooth epoxidation should occur for **3** but not for **2**. In reality, better reactivity was observed for **2**, contrary to our expectation.

Table 1. Competitive epoxidation reactions between **2** and **3**.^[a,b]

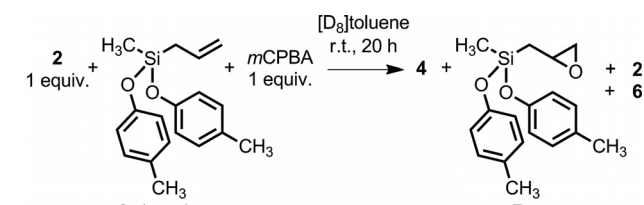
		solvent r.t., 20 h			
		$\xrightarrow[\text{1 equiv.}]{\text{2 (1 equiv.) + 3 (1 equiv.) + mCPBA (1 equiv.)}}$			
Entry	Solvent	Yield [%] ^[c]			
		4	5	2	3
1	$[\text{D}_6]\text{benzene}$	27	17	24	32
2	$[\text{D}_8]\text{toluene}$	32	23	19	26
3	$[\text{D}_{10}]\text{-}p\text{-xylene}$	31	18	19	32
4 ^[d]	$[\text{D}_{12}]\text{mesitylene}$	≈ 0 ^[e]	≈ 0 ^[e]	≈ 50	≈ 50

[a] Conditions: **2** (0.02 mmol, 31 mg), **3** (0.02 mmol, 31 mg), and *m*CPBA (0.02 mmol, 5 mg) with the deuterated solvent (0.5 mL) in an NMR tube. [b] All of the starting *m*CPBA (1 equiv.) was consumed. [c] Determined by ^1H NMR spectroscopy. [d] Many signals were too broad to assign: C_9D_{12} does not fit for each cavity of **2** and **3**. [e] No reaction was observed by TLC analysis, and starting **2** and **3** remained.

Given the observed reactivity of **2**, we worked on competitive reactions between **2** and **6** (Table 2). Compound **6** was derived from *p*-cresol, and it is sterically unhindered relative to **2**. Less-congested **6** should undergo faster epoxidation than **4** to afford **7**; however, surprisingly, the ratio of **7/4** was nearly the same: 26:24. The competition proved that the reactivity of encumbered allyl **2** was comparable to that of unfortified allyl **6**. The results in Tables 1 and 2 suggest that well-arrayed quinoxalines of **2** do not merely hin-

der the oxidation process; that is, the magnetic environment inside the cavity promotes the reaction. This is supported by the result of entry 4 in Table 1: no epoxidation proceeded in $[\text{D}_{12}]\text{mesitylene}$, and **2** and **3** remained untouched.^[18] $[\text{D}_{12}]\text{mesitylene}$ is larger in size than $[\text{D}_{10}]\text{-}p\text{-xylene}$, $[\text{D}_8]\text{-toluene}$, and $[\text{D}_6]\text{benzene}$, and thus it cannot fit inside the cavity; in fact, the signals in the ^1H NMR spectra of **2** and **3** in $[\text{D}_{12}]\text{mesitylene}$ are too broad to assign.^[19] The quinoxaline substructures in mesitylene are not arranged in a fixed order to equilibrate between the vase and kite form, and consequently, the floating quinoxalines sterically hinder each allyl group in **2** and **3** and stop the epoxidation.

Table 2. A competitive epoxidation reaction between **2** and **6**.^[a,b]

				
Yield [%] ^[c]				
4	7	2	6	
26	24	25	25	

[a] Conditions: **2** (0.02 mmol, 31 mg), **6** (0.02 mmol, 6 mg), and *m*CPBA (0.02 mmol, 5 mg) in $[\text{D}_8]\text{toluene}$ (0.5 mL) in an NMR tube. [b] All of the starting *m*CPBA (1 equiv.) was consumed. [c] Determined by ^1H NMR spectroscopy.

How does the vase-shaped cavity enhance the reactivity beyond steric hindrance? Its dense π -orbital space could delocalize electrons that interchange between the allyl group and *m*CPBA during the course of the reaction. Thus, the cavity stabilizes the process and reduces the enthalpic price of the reaction. The reactants are confined in a limited space and are properly placed, and the desired reactive species would be actively stabilized.^[20]

Conclusions

In summary, we have successfully inserted a reactive allyl group inside cavitand **1**, and its magnetic environment inside the capsule proved to be unusual because of the many aromatic rings that enclose it. The NMR signals of the encapsulated allyl are thus profoundly altered relative to those of the outward allyl, and so it is easily distinguished from its unrestrained counterparts. The introverted allyl underwent *m*CPBA-mediated epoxidation and unexpectedly showed higher reactivity than the extroverted allyl. Through examination in $[\text{D}_{12}]\text{mesitylene}$ and a competitive experiment with small allyl **6**, a remarkably salient feature was revealed in the vase form, which is capable of holding the reactive allyl moiety. Further synthetic development of functionalized cavitands is ongoing and will be reported in due course.

Experimental Section

Synthesis of Cavitand 2 and 3: Under an argon atmosphere, a two-necked flask was charged with **1** (1 mmol, 1.48 g), triethylamine (2.4 mmol, 0.33 mL), and anhydrous toluene (20 mL). Allyl(dichloro)methylsilane (1.1 mmol, 0.16 mL) was then added. After stirring at ambient temperature for 2 h, the reaction mixture was filtered through a pad of cotton and concentrated in vacuo to give the crude products as white solid materials. Purification by silica gel column chromatography (hexane/ethyl acetate 9:1) yielded target **2** (533 mg, 34%) as a white solid material and **3** (417 mg, 27%) as a white solid material. Data for **2**: Yield 34% (533 mg), white solid. ^1H NMR (400 MHz, CDCl_3): δ = 8.28 (s, 2 H), 7.92–7.84 (m, 4 H), 7.67 (d, J = 8.2 Hz, 2 H), 7.55–7.44 (m, 6 H), 7.33 (s, 2 H), 7.18 (s, 2 H), 7.16 (s, 2 H), 5.76 (t, J = 8.1 Hz, 1 H), 5.68 (t, J = 8.0 Hz, 2 H), 5.41 (ddt, J = 17.1, 10.1, 8.0 Hz, 1 H, $\text{SiCH}_2\text{CH}=\text{CH}_2$), 4.82 (d, J = 10.1 Hz, 1 H, $\text{SiCH}_2\text{CH}=\text{CH}_2$), 4.62 (d, J = 17.1 Hz, 1 H, $\text{SiCH}_2\text{CH}=\text{CH}_2$), 4.54 (t, J = 7.9 Hz, 1 H), 2.34–2.19 (m, 8 H), 1.47–1.29 (m, 72 H), 0.96–0.85 (m, 12 H), 0.81 (d, J = 8.0 Hz, 2 H, $\text{SiCH}_2\text{CH}=\text{CH}_2$), 0.47 (s, 3 H, SiCH_3) ppm. ^{13}C NMR (100 MHz, CDCl_3): δ = 8.71 (s, 2 H), 8.00 (d, J = 8.2 Hz, 2 H), 7.76 (s, 2 H), 7.67 (d, J = 8.2 Hz, 2 H), 7.63 (s, 2 H), 7.54 (dd, J = 6.3, 3.4 Hz, 2 H), 7.47 (s, 2 H), 7.24 (dd, J = 8.2, 8.2 Hz, 2 H), 7.12–7.04 (m, 4 H), 6.16 (t, J = 8.2 Hz, 2 H), 6.05 (t, J = 8.2 Hz, 1 H), 4.94 (ddt, J = 17.0, 10.5, 8.0 Hz, 1 H, $\text{SiCH}_2\text{CH}=\text{CH}_2$), 4.74 (t, J = 8.0 Hz, 1 H), 4.58 (dd, J = 10.5, 2.0 Hz, 1 H, $\text{SiCH}_2\text{CH}=\text{CH}_2$), 4.10 (dd, J = 17.0, 2.0 Hz, 1 H, $\text{SiCH}_2\text{CH}=\text{CH}_2$), 2.50–2.32 (m, 8 H), 1.57–1.29 (m, 72 H), 0.96–0.93 (m, 12 H), 0.28 (s, 3 H, SiCH_3), –0.13 (d, J = 8.0 Hz, 2 H, $\text{SiCH}_2\text{CH}=\text{CH}_2$) ppm. ^{13}C NMR (100 MHz, CDCl_3): δ = 153.3, 153.1, 153.0, 152.9, 152.7, 152.6, 150.3, 140.2, 140.08, 140.06, 136.9, 136.3, 134.6, 133.0, 131.6, 129.7, 129.6, 129.4, 128.15, 128.11, 127.9, 124.2, 123.0, 119.0, 116.1, 115.8, 35.4, 34.5, 34.3, 32.9, 32.7, 32.3 (many peaks are overlapped), 30.1 (many peaks are overlapped), 29.8 (many peaks are overlapped), 28.4, 23.1 (many peaks are overlapped), 19.7, 14.5 (many peaks are overlapped), –4.7 ppm. MS (FAB): m/z = 1567 $[\text{M}+\text{H}]^+$. IR (neat): $\tilde{\nu}$ = 2921, 2850, 1482, 1414, 1331, 1158 cm^{-1} . $\text{C}_{100}\text{H}_{124}\text{N}_6\text{O}_8\text{Si}$ (1566.20): calcd. C 76.69, H 7.98, N 5.37; found C 76.79, H 7.90, N 5.01. Data for **3**: Yield 27% (417 mg), white solid. ^1H NMR (400 MHz, CDCl_3): δ = 8.26 (s, 2 H), 7.90–7.85 (m, 4 H), 7.66 (d, J = 8.2 Hz, 2 H), 7.55–7.43 (m, 6 H), 7.30 (s, 2 H), 7.14 (s, 2 H), 7.12 (s, 2 H), 5.94 (ddt, J = 17.0, 10.1, 7.8 Hz, 1 H, $\text{SiCH}_2\text{CH}=\text{CH}_2$), 5.73 (t, J = 8.0 Hz, 1 H), 5.65 (t, J = 8.1 Hz, 2 H), 5.11 (d, J = 17.0 Hz, 1 H, $\text{SiCH}_2\text{CH}=\text{CH}_2$), 5.06 (d, J = 10.1 Hz, 1 H, $\text{SiCH}_2\text{CH}=\text{CH}_2$), 4.55 (t, J = 7.8 Hz, 1 H), 2.35–2.19 (m, 8 H), 1.94 (d, J = 7.8 Hz, 2 H, $\text{SiCH}_2\text{CH}=\text{CH}_2$), 1.45–1.29 (m, 72 H), 0.94–0.84 (m, 12 H), –0.56 (s, 3 H, SiCH_3) ppm. ^{13}C NMR (100 MHz, CDCl_3): δ = 8.69 (s, 2 H), 7.97 (d, J = 8.0 Hz, 2 H), 7.73 (s, 2 H), 7.61–7.56 (m, 6 H), 7.43 (s, 2 H), 7.24 (dd, J = 7.2, 7.2 Hz, 2 H), 7.09–7.06 (m, 4 H), 6.14 (t, J = 8.1 Hz, 2 H), 6.05 (t, J = 8.1 Hz, 1 H), 5.81 (ddt, J = 17.5, 9.4, 7.8 Hz, 1 H, $\text{SiCH}_2\text{CH}=\text{CH}_2$), 4.95 (m, 2 H, $\text{SiCH}_2\text{CH}=\text{CH}_2$, two peaks are overlapped), 4.77 (t, J = 7.9 Hz, 1 H), 2.47–2.34 (m, 8 H), 1.66 (d, J = 7.8 Hz, 2 H, $\text{SiCH}_2\text{CH}=\text{CH}_2$), 1.48–1.29 (m, 72 H), 0.99–0.89 (m, 12 H), –1.32 (s, 3 H, SiCH_3) ppm. ^{13}C NMR (100 MHz, CDCl_3): δ = 153.3, 153.2, 153.0, 152.9, 152.7, 152.6, 150.4, 140.13, 140.11, 140.05, 136.9, 136.3, 134.7, 132.9, 131.8, 129.6, 129.5, 129.3, 128.2, 128.1, 127.9, 124.2, 123.0, 118.9, 116.2, 116.0, 35.2, 34.6, 34.3, 32.8, 32.7, 32.3 (many peaks are overlapped), 30.1 (many peaks are overlapped), 29.8 (many peaks are overlapped), 28.4, 23.1 (many peaks are overlapped), 21.7, 14.5 (many peaks are overlapped), –6.2 ppm. MS (FAB): m/z = 1567 $[\text{M}+\text{H}]^+$. IR (neat): $\tilde{\nu}$ = 2120, 2850, 1481, 1404, 1331,

1153 cm^{-1} . $\text{C}_{100}\text{H}_{124}\text{N}_6\text{O}_8\text{Si}$ (1566.20): calcd. C 76.69, H 7.98, N 5.37; found C 76.32, H 7.96, N 5.02.

Supporting Information (see footnote on the first page of this article): General procedures and characterization data of new compounds.

Acknowledgments

The authors are pleased to thank Dr. Fukashi Matsumoto at OMTRI for assistance with MALDI-MS. Professor Michael P. Schramm at CSULB is thanked for helpful discussions.

- [1] a) J. A. Gerlt, *Chem. Rev.* **1987**, *87*, 1079–1105; b) J. C. M. van Hest, D. A. Tirrel, *Chem. Commun.* **2001**, 1897–1904; c) M. V. Rodnina, W. Wintermeyer, *Curr. Opin. Struct. Biol.* **2003**, *13*, 334–340; d) K. Shen, A. C. Hines, D. Schwarzer, K. A. Pickin, P. A. Cole, *Biochim. Biophys. Acta Proteins Proteomics* **2005**, *1754*, 65–78.
- [2] a) G. Varani, *Annu. Rev. Biophys. Biomol. Struct.* **1995**, *24*, 379–404; b) V. J. DeRose, *Curr. Opin. Struct. Biol.* **2003**, *13*, 317–324; c) S. Shuman, C. D. Lima, *Curr. Opin. Struct. Biol.* **2004**, *14*, 757–764.
- [3] a) A. J. Skerra, *J. Mol. Recognit.* **2000**, *13*, 167–187; b) G. Folkers, C. D. P. Klein, *Angew. Chem. Int. Ed.* **2001**, *40*, 4175–4177; *Angew. Chem.* **2001**, *113*, 4303–4305; c) C. Khosla, P. B. Harbury, *Nature* **2001**, *409*, 247–252; d) T. C. Bruice, *Acc. Chem. Res.* **2002**, *35*, 139–148.
- [4] a) J. R. Moran, S. Karbach, D. J. Cram, *J. Am. Chem. Soc.* **1982**, *104*, 5826–5828; b) D. J. Cram, *Science* **1983**, *219*, 1177–1183; c) J. R. Moran, J. L. Ericson, E. Dalcanele, J. A. Bryant, C. B. Knobler, D. J. Cram, *J. Am. Chem. Soc.* **1991**, *113*, 5707–5714; d) D. J. Cram, J. M. Cram, *Container Molecules and Their Guests*, Royal Society of Chemistry, Cambridge, **1994**, p. 85–130.
- [5] a) P. Timmerman, M. G. A. van Mook, W. Verboom, G. J. van Hummel, S. Harkema, D. N. Reinhoudt, *Tetrahedron Lett.* **1992**, *33*, 3377–3380; b) P. Timmerman, H. Boerrigter, W. Verboom, G. J. van Hummel, S. Harkema, D. N. Reinhoudt, *J. Inclusion Phenom. Mol. Recognit. Chem.* **1994**, *19*, 167–191; c) P. Timmerman, W. Verboom, D. N. Reinhoudt, *Tetrahedron* **1996**, *52*, 2663–2704; d) H. Boerrigter, W. Verboom, G. J. van Hummel, S. Harkema, D. N. Reinhoudt, *Tetrahedron Lett.* **1996**, *37*, 5167–5170.
- [6] a) T. N. Sorrell, F. C. J. Pigge, *Org. Chem.* **1993**, *58*, 784–785; b) T. Haino, T. Harano, K. Matsumura, Y. Fukazawa, *Tetrahedron Lett.* **1995**, *36*, 5793–5796; c) T. Haino, K. Matsumura, T. Harano, K. Yamada, Y. Saijyo, Y. Fukazawa, *Tetrahedron* **1998**, *54*, 12185–12196; d) J. L. Irwin, M. S. Sherbum, *J. Org. Chem.* **2000**, *65*, 602–605; e) T. Haino, M. Kobayashi, M. Chikaraishi, Y. Fukazawa, *Chem. Commun.* **2005**, *18*, 2321–2323.
- [7] a) D. M. Rudkevich, J. Rebek Jr., *Eur. J. Org. Chem.* **1999**, 1991–2005; b) T. Haino, D. M. Rudkevich, A. Shivanyuk, K. Rissanen, J. Rebek Jr., *Chem. Eur. J.* **2000**, *6*, 3797–3805; c) B. W. Purse, J. Rebek Jr., *Proc. Natl. Acad. Sci. USA* **2005**, *102*, 10777–10782.
- [8] A. R. Renslo, J. Rebek Jr., *Angew. Chem. Int. Ed.* **2000**, *39*, 3281–3283; *Angew. Chem.* **2000**, *112*, 3419–3421.
- [9] B. W. Purse, P. Ballester, J. Rebek Jr., *J. Am. Chem. Soc.* **2003**, *125*, 14682–14683.
- [10] A. Gissot, J. Rebek Jr., *J. Am. Chem. Soc.* **2004**, *126*, 7424–7425.
- [11] a) T. Iwasawa, R. J. Hooley, J. Rebek Jr., *Science* **2007**, *317*, 493–496; b) T. Iwasawa, P. L. Wash, C. Gibson, J. Rebek Jr., *Tetrahedron* **2007**, *63*, 6506–6511; c) R. J. Hooley, T. Iwasawa, J. Rebek Jr., *J. Am. Chem. Soc.* **2007**, *129*, 15330–15339; d) R. J. Hooley, P. Restorp, T. Iwasawa, J. Rebek Jr., *J. Am. Chem. Soc.* **2007**, *129*, 15639–15643.

- [12] a) S. M. Butterfield, J. Rebek Jr., *J. Am. Chem. Soc.* **2006**, *128*, 15366–15367; b) P. L. Wash, A. R. Renslo, J. Rebek Jr., *Angew. Chem. Int. Ed.* **2001**, *40*, 1221–1222; *Angew. Chem.* **2001**, *113*, 1261–1262.
- [13] a) B. Benmerad, P. Clair, D. Armspach, D. Matt, F. Balegroune, L. Toupet, *Chem. Commun.* **2006**, 2678–2680; b) K. Goto, M. Holler, R. Okazaki, *J. Am. Chem. Soc.* **1997**, *119*, 1460–1461; c) S. Watanabe, K. Goto, T. Kawashima, R. Okazaki, *Tetrahedron Lett.* **1995**, *36*, 7677–7680; d) T. K. Park, J. Schroeder, J. Rebek Jr., *J. Am. Chem. Soc.* **1991**, *113*, 5125–5127.
- [14] P. P. Castro, G. Zhao, G. A. Masangkay, C. Hernandez, L. M. Gutierrez-Tunstad, *Org. Lett.* **2004**, *6*, 333–336.
- [15] This observation is in agreement with the vase–kite switching systems, as studied by Diederich and co-workers, in which a class of quinoxaline-spanned cavitands was strongly apt to form the vase in aromatic solvents, see: A. V. Azov, B. Jaun, F. Diederich, *Helv. Chim. Acta* **2004**, *87*, 449–462.
- [16] T. Iwasawa, Y. Nishimoto, K. Hama, T. Kamei, M. Nishiuchi, Y. Kawamura, *Tetrahedron Lett.* **2008**, *49*, 4758–4762.
- [17] Differences in reaction rates between these solvents were not particularly observed.
- [18] Smooth epoxidation of allyl **6** in [D₁₂]mesitylene was ensured.
- [19] a) T. Heinz, D. Rudkevich, J. Rebek Jr., *Nature* **1998**, *394*, 764–766; b) T. Heinz, D. Rudkevich, J. Rebek Jr., *Angew. Chem. Int. Ed.* **1999**, *38*, 1136–1139; *Angew. Chem.* **1999**, *111*, 1206–1209.
- [20] A. Fersht, *Enzyme Structure and Mechanism*, Freeman, New York, **1984**, p. 47–97.

Received: December 11, 2013

Published Online: February 6, 2014